

THE PROTOSTAR IN THE MASSIVE INFRARED DARK CLOUD IRDC18223-3

H. BEUTHER¹ & J. STEINACKER^{1,2}
beuther@mpia.de, stein@mpia.de*Accepted for ApJL on 5th of January 2007, Draft version from July 24, 2021*

ABSTRACT

At the onset of high-mass star formation, accreting protostars are deeply embedded in massive cores made of gas and dust. Their spectral energy distribution is still dominated by the cold dust and rises steeply from near-to far-infrared wavelengths. The young massive star-forming region IRDC 18223-3 is a prototypical Infrared-Dark-Cloud with a compact mm continuum core that shows no protostellar emission below $8\mu\text{m}$. However, based on outflow tracers, early star formation activity was previously inferred for this region. Here, we present recent Spitzer observations from the MIPSGAL survey that identify the central protostellar object for the first time at 24 and $70\mu\text{m}$. Combining the mid- to far-infrared data with previous mm continuum observations and the upper limits below $8\mu\text{m}$, one can infer physical properties of the central source. At least two components with constant gas mass M and dust temperature T are necessary: one cold component ($\sim 15\text{ K}$ and $\sim 576\text{ M}_\odot$) that contains most of the mass and luminosity, and one warmer component ($\geq 51\text{ K}$ and $\geq 0.01\text{ M}_\odot$) to explain the $24\mu\text{m}$ data. The integrated luminosity of $\sim 177\text{ L}_\odot$ can be used to constrain additional parameters of the embedded protostar from the turbulent core accretion model for massive star formation. The data of IRDC 18223-3 are consistent with a massive gas core harboring a low-mass protostellar seed of still less than half a solar mass with high accretion rates of the order $10^{-4}\text{ M}_\odot\text{ yr}^{-1}$. In the framework of this model, the embedded protostar is destined to become a massive star at the end of its formation processes.

Subject headings: stars: formation – stars: individual (IRDC 18223-3) – stars: early-type – infrared: general

1. INTRODUCTION

The onset of massive star formation was elusive to observational research until recently. Very young regions of massive star formation contain large amounts of cold gas and dust observable from far-infrared (FIR) to mm wavelengths. A possibly luminous embedded object has not yet formed or is obscured by the large optical depth of the surrounding cold dust at near-/mid-infrared wavelengths (NIR/MIR). The advent of the Infrared Space Observatory (ISO) and the Midcourse Space Experiment (MSX) allowed to identify large numbers of such Infrared Dark Clouds (IRDCs) (Egan et al. 1998; Bacmann et al. 2000; Carey et al. 2000; Simon et al. 2006). However, the IRDCs are not a well defined class, but these clouds are expected to harbor various evolutionary stages. Adopting the evolutionary sequence outlined in Beuther et al. (2006), IRDCs should be capable to contain genuine High-Mass Starless Cores (HMSCs), High-Mass Cores harboring accreting Low-/Intermediate-Mass Protostars, and the youngest High-Mass Protostellar Objects (HMPOs). While the first group is important to study the physical conditions of massive cores before the onset of star formation, the latter two stages are essential to understand the early evolution in massive star formation. Since the evolutionary timescale to form high-mass stars is short (of the order 10^5 yr , e.g., McKee & Tan 2002), and the central evolving protostars are deeply embedded within their natal cores, observational discrimination between these different

evolutionary stages of IRDCs is a challenging task.

Recently, Beuther et al. (2005) observed with the Plateau de Bure Interferometer (PdBI) a filamentary IRDC containing a compact 3.2 mm continuum peak related to a massive core that remains undetected in the SPITZER GLIMPSE survey up to $8\mu\text{m}$ (Fig. 1, left panel). Based on the GLIMPSE non-detection one could speculate that this may be a genuine HMSC, however, there are additional indicators leading in the opposite direction. The Spitzer $4.5\mu\text{m}$ band shows weak emission right at the edge of the 3.2 mm continuum core. This so-called green-fuzzy emission is usually attributed to shock-excited H_2 emission which is especially prominent in this band (Noriega-Crespo et al. 2004). Such H_2 features can be attributed to early outflow activity. This scenario is supported by single-dish CO and CS spectra showing non-Gaussian line-wing emission indicative of molecular outflows. Furthermore, $\text{NH}_3(1,1)$ and $(2,2)$ inversion line observations revealed relatively high gas temperatures of the order 33 K which would not be expected in the case of a starless core. Therefore, Beuther et al. (2005) argue that we are witnessing the onset of massive star formation. Based on the outflow signatures and the high NH_3 temperatures, a central protostar should have formed already, but it must still be in a very early evolutionary stage to remain undetected up to $8\mu\text{m}$. The detection of at least three $4.5\mu\text{m}$ outflow features indicates that even a multiple system may be embedded in this core. At a temperature of 33 K and a distance of $\sim 3.7\text{ kpc}$ (Sridharan et al. 2002,

¹ Max-Planck-Institute for Astronomy, Königstuhl 17, 69117 Heidelberg, Germany² Astronomisches Recheninstitut am Zentrum für Astronomie Heidelberg, Mönchhofstr. 12-14, 69120 Heidelberg, Germany³ The near kinematic distance was chosen because IRDC at $>12\text{ kpc}$ are unlikely to be observable. The kinematic distance uncertainty is of the order 1 kpc (Brand & Blitz 1993).

2005³), Beuther et al. (2005) calculated from the 3.2 mm continuum flux a mass and column density of the gas core of $\sim 184 M_{\odot}$ and $\sim 10^{24} \text{ cm}^{-2}$ ($A_v \sim 1000$).

In the framework of the above mentioned evolutionary sequence, IRDC 18223-3 should be part of the High-Mass Cores harboring accreting Low-/Intermediate-Mass Protostars. For such a source, it is expected that the spectral energy distribution (SED) rises sharply at mid- to far-infrared wavelength and should hence become detectable there. The newly released Spitzer legacy survey MIPS-GAL (MIPS Inner Galactic Plane Survey) is the ideal resource to search for such MIR/FIR emission and study this young source in more detail.

2. DATA

The MIPS 24 and 70 μm data were taken from the Spitzer archive of the recently released MIPSGAL survey (Carey et al. 2005). Fluxes were extracted via aperture photometry subtracting the background emission from a close-by region. The Spitzer IRAC 3.5 to 8 μm and the PdBI 3.2 mm continuum data were first presented in Beuther et al. (2005). Furthermore, we use a 1.2 mm continuum flux measurement observed with the IRAM 30 m telescope (Beuther et al. 2002). For the 3.2 mm data, we use the flux within the 50% contour level (radius of $\sim 10000 \text{ AU}$) to avoid contamination from the large-scale filament. Similarly, for the 1.2 mm data we use the peak flux measurement within the central 11" beam. Beuther et al. (2005) estimated for the whole large-scale filamentary structure that the PdBI observations suffer from about 25% of missing flux. However, since here we are not interested in the whole filament but only analyze the flux from the central compact peak-emission, this effect is considerably lower. The accuracy of the flux measurements at mm wavelength is estimated from the data to be correct within $\sim 15\%$ and for the 24 and 70 μm within 20%. The 3σ upper limits of the four Spitzer IRAC datasets are 0.05 mJy at 3.6 and 4.5 μm , 0.13 mJy at 5.8 μm and 0.15 at 8 μm (Beuther et al. 2005).

3. RESULTS

Figure 1 presents overlays of the MIPS/IRAC mid-/far-infrared data and the 3.2 mm observations. The most striking result is that the 3.2 mm core, which is dark at least up to 8 μm , is now detected in the 24 and 70 μm bands. Previously, we could only indirectly infer from outflow indicators and warm gas temperatures that the core likely harbors already a very young protostar, but the new 24 and 70 μm data clearly identify this source now for the first time shortward of 100 μm .

Combining the 3.2 and 1.2 mm data from the Rayleigh-Jeans part of the spectrum with the 24 and 70 μm fluxes on the Wien-side of the SED, this dataset allows to derive the physical properties of this High-Mass Core at the onset of massive star formation in more detail. Table 1 presents the fluxes from 24 μm to 3.2 mm, and Figure 2 shows the resulting SED.

The spectral energy distribution was fitted with Planck black-body functions accounting for the wavelength-dependent emissivity of the dust. The assumed dust composition follows Draine & Lee (1984). As a first order approach, we tried to fit the dataset with a single-component

black-body function. While this may work for the measurements upwards of 70 μm , the 24 μm point shows significant excess emission to a single-component fit, and a second warmer component has to be added. Figure 2 presents a two-component fit to the data. While most of the flux, mass and luminosity stems from the cold gas and dust with an approximate temperature of 15 K, we find another warm component with a temperature around ≥ 51 K. The gas masses associated with the cold and warm components are ~ 576 and $\geq 0.01 M_{\odot}$, respectively. Since on the Wien-side of the SED the emission is not optically thin anymore, we consider the masses and temperatures of the warm component as lower limits. The mass difference of the cold component between the new fit and the older mass estimates from Beuther et al. (2005) are due to the lower dust temperature we now derive (15 K versus 33 K from the NH₃ gas observations) and the different assumptions about the dust grain size distributions (following now Draine & Lee 1984, whereas previously we used the approach by Hildebrand 1983). Furthermore, the integrated luminosity one derives from this two-component fit is $\sim 177 L_{\odot}$ (174 and 3 L_{\odot} in the cold and warm component, respectively).

4. DISCUSSION

Although, we cannot fit the 24 μm flux measurements without the additional warmer component, it is clear that this component does not contribute significantly to the mass and luminosity of the region. In the regime of low-mass star formation, recently there have been several detections of very-low-luminosity objects (VeLLOs) within previously believed starless cores (Young et al. 2004; Dunham et al. 2006; Bourke et al. 2006). Some of these objects show clear outflow signatures (L1014, Bourke et al. 2005; IRAM04191+1522, Dunham et al. 2006), and they are believed to be very young low-mass protostars or brown dwarfs likely associated with accretion disks. In the case of IRDC 18223-3, the region exhibits outflow signatures as well (Beuther et al. 2005), hence it is likely that the warm component in this source is produced by an accreting low-mass protostar-disk system as well. An important difference between the VeLLOs and IRDC 18223-3 is that the luminosity of the warm component in IRDC 18223-3 – although it is nearly negligible compared to the luminosity of the cold component – is about 1-2 orders larger than those of the VeLLOs. Since we are dealing with a massive gas core that has on average still very low temperatures and a low total luminosity, IRDC 18223-3 is a good candidate of being a High-Mass Core with an embedded low- to intermediate mass protostar that is destined to become a massive star at the end of its formation processes.

To constrain the status of the embedded source in more detail, we compare our data with the analytic and the radiation-hydrodynamic simulations of the turbulent core model for massive star formation (McKee & Tan 2002, 2003; Krumholz et al. 2006). At early evolutionary stages prior to any hydrogen or even deuterium burning, the luminosity of the regions is completely dominated by the accretion luminosity caused by the accretion shocks. The theoretical results obtained by the analytic approach of McKee & Tan (2003) and the simulations of

Krumholz et al. (2006) resemble each other well. Some quantitative relatively small differences are due to different assumptions in the initial density distributions, different turbulence damping assumptions and the origin of the core in a shocked filament in the simulations which delay all result in higher accretion rates in the radiative-hydrodynamic simulations. Since the latter likely resemble real cores better, we use the simulations for our comparison.

Figure 5 in Krumholz et al. (2006) presents the accretion rate and luminosity of the forming massive protostar throughout its evolution. A notable difference between the simulations and our observations is that the simulated luminosity is only that of the primary protostar, whereas the estimated luminosity of IRDC 18223-3 includes likely multiple objects as well as potential contributions from external heating. However, since there is no detected UCHII region or strong O-star within several pc from IRDC 18223-3, external heating contributions should be negligible. Since massive star formation is usually proceeding in a clustered mode, multiple embedded protostars below our current angular resolution limit ($5.8'' \times 2.4''$ at 3 mm wavelength corresponding to approximately 15000 AU, Beuther et al. 2005) cannot be excluded. Nevertheless, it is likely that the luminosity of the region will be dominated by the most massive protostellar object which is also confirmed by the simulations of Krumholz et al. (2006). Therefore, it appears reasonable to compare these simulations with our observational results.

The luminosity obtained for IRDC 18223-3 is reached in the simulations by Krumholz et al. (2006) already at extremely early times when the protostellar mass is still well below half a solar mass. The corresponding accretion rates are of the order $10^4 M_\odot \text{ yr}^{-1}$. Therefore, combining the model predictions with the observed properties of this region indicates that we are really dealing with a massive gas core that harbors an embedded, accreting low-mass

protostar with accretion rates that are high enough that it will eventually form a massive star.

Although the data do not allow us to unambiguously exclude that the embedded low-mass protostar may remain a low-mass object potentially never forming a massive star, the fact that the gas core is very massive, and that the luminosity is already relatively high (a genuine low-mass protostar has orders of magnitude lower accretion rates and hence a significantly lower accretion luminosity), strongly supports the proposed scenario of a massive star-forming region right at the onset of protostellar evolution and accretion.

The example of IRDC 18223-3 shows the power of combining (sub)mm high-spatial-resolution observations with the recently available near-/mid-/and far-infrared surveys of the Galactic plane by Spitzer. Combining these datasets allows us to constrain the SEDs of the youngest massive star-forming regions in unprecedented detail. This way we can observationally characterize the various evolutionary stages right at the beginning of massive star formation, in particular the largely unknown properties of genuine high-mass starless cores and high-mass cores harboring low- to intermediate-mass protostars like the case of IRDC 18223-3. We are currently performing radiative transfer modeling that incorporates age estimates based on the emerging MIR flux but this is out of the scope of the current paper. For the coming years we can expect studies of larger IRDC samples setting constraints on the source properties in a statistical sense.

SPITZER is operated by JPL, Caltech under NASA contract 1407. We acknowledge H. Linz, J. Bouwman and S. Quanz for help with the SPITZER MIPS data. H.B. acknowledges financial support by the Emmy-Noether-Programm of the Deutsche Forschungsgemeinschaft (DFG, grant BE2578).

REFERENCES

Bacmann, A., André, P., Puget, J.-L., et al. 2000, A&A, 361, 555
 Beuther, H., Churchwell, E., McKee, C., & Tan, J. 2006, in PPV, astro-ph/0511294
 Beuther, H., Schilke, P., Menten, K. M., et al. 2002, ApJ, 566, 945
 Beuther, H., Sridharan, T. K., & Saito, M. 2005, ApJ, 634, L185
 Bourke, T. L., Crapsi, A., Myers, P. C., et al. 2005, ApJ, 633, L129
 Bourke, T. L., Myers, P. C., Evans, II, N. J., et al. 2006, ApJ, 649, L37
 Brand, J. & Blitz, L. 1993, A&A, 275, 67
 Carey, S. J., Feldman, P. A., Redman, R. O., et al. 2000, ApJ, 543, L157
 Carey, S. J., Noriega-Crespo, A., Price, S. D., et al. 2005, American Astronomical Society Meeting Abstracts, 207, 63.33
 Draine, B. T. & Lee, H. M. 1984, ApJ, 285, 89
 Dunham, M. M., Evans, II, N. J., Bourke, T. L., et al. 2006, ApJ, 651, 945
 Egan, M. P., Shipman, R. F., Price, S. D., et al. 1998, ApJ, 494, L199
 Hildebrand, R. H. 1983, QJRAS, 24, 267
 Krumholz, M., Klein, R., & McKee, C. 2006, ArXiv Astrophysics e-prints: astro-ph/0609798
 McKee, C. F. & Tan, J. C. 2002, Nature, 416, 59
 —. 2003, ApJ, 585, 850
 Noriega-Crespo, A., Morris, P., Marleau, F. R., et al. 2004, ApJS, 154, 352
 Simon, R., Jackson, J. M., Rathborne, J. M., & Chambers, E. T. 2006, ApJ, 639, 227
 Sridharan, T. K., Beuther, H., Saito, M., Wyrowski, F., & Schilke, P. 2005, ApJ, 634, L57
 Sridharan, T. K., Beuther, H., Schilke, P., Menten, K. M., & Wyrowski, F. 2002, ApJ, 566, 931
 Young, C. H., Jørgensen, J. K., Shirley, Y. L., et al. 2004, ApJS, 154, 396

FIG. 1.— The color scales show Spitzer images at various wavelength. The left panel presents a three-color composite with blue $3.6 \mu\text{m}$, green $4.5 \mu\text{m}$, red $8.0 \mu\text{m}$ (adapted from Beuther et al. 2005). The inlay zooms into the central core region. The middle and right panel show the Spitzer 24 and $70 \mu\text{m}$ images, respectively. The scaling is chosen individually to highlight the most prominent structures. Contours in each panel show the 93 GHz (3.2 mm) continuum emission observed with the PdBI from $1.08 \text{ mJy beam}^{-1}$ (3σ) in $0.72 \text{ mJy beam}^{-1}$ (2σ) steps (Beuther et al. 2005). The axes are in R.A (J2000.0) and decl. (J2000.0). The circles in each panel present the Spitzer beam sizes and the ellipse in the left panel presents the PdBI 3.2 mm continuum synthesized beam. A size-ruler is also shown in the left panel.

TABLE 1

FLUXES

λ μm	S mJy
24	12.1 ± 2.4
70	989 ± 198
1200	290 ± 44
3200	6.7 ± 1.0

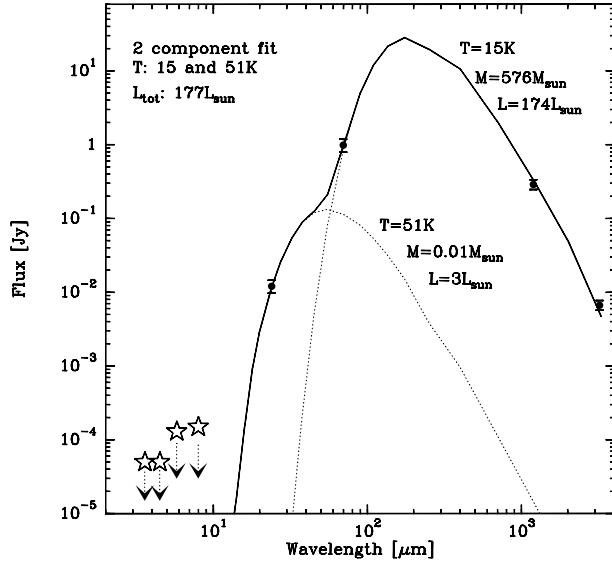


FIG. 2.— Spectral energy distribution of IRDC 18223-3. The dots with error-bars mark the detections at 24 and 70 μm on the short-wavelength Wien-side of the peak, and at 1.2 and 3.2 mm on the Rayleigh-Jeans part of the spectrum. The four stars below 10 μm show the Spitzer IRAC upper limits in the near-infrared. The solid line presents a two-component fit with one cold component at $\sim 15\text{ K}$ and one warmer component at $\sim 51\text{ K}$. The two dotted lines show the two components separately. The resulting physical parameters for each component are labeled accordingly.

This figure "f1.jpg" is available in "jpg" format from:

<http://arxiv.org/ps/astro-ph/0701185v1>